

Article

Optimized Artificial Intelligent Model to Boost the Efficiency of Saline Wastewater Treatment Based on Hunger Games Search Algorithm and ANFIS

Hegazy Rezk ^{1,2} , Abdul Ghani Olabi ^{3,4,*}, Enas Taha Sayed ^{3,5}, Samah Ibrahim Alshathri ^{6,*} 
and Mohammad Ali Abdelkareem ^{3,5} 

- ¹ Department of Electrical Engineering, College of Engineering in Wadi Alldawasir, Prince Sattam bin Abdulaziz University, Wadi Alldawasir 11991, Saudi Arabia
 - ² Department of Electrical Engineering, Faculty of Engineering, Minia University, Minia 61111, Egypt
 - ³ Sustainable Energy and Power Systems Research Centre, RISE, University of Sharjah, Sharjah P.O. Box 27272, United Arab Emirates
 - ⁴ Mechanical Engineering and Design, School of Engineering and Applied Science, Aston University, Aston Triangle, Birmingham B4 7ET, UK
 - ⁵ Chemical Engineering Department, Faculty of Engineering, Minia University, Minia 61111, Egypt
 - ⁶ Department of Information Technology, College of Computer and Information Sciences, Princess Nourah bint Abdulrahman University, P.O. Box 84428, Riyadh 11671, Saudi Arabia
- * Correspondence: aolabi@sharjah.ac.ae (A.G.O.); sealshathry@pnu.edu.sa (S.I.A.)

Abstract: Chemical oxygen demand (COD) and total organic carbon (TOC) removal efficiencies of saline wastewater treatment indicate the efficiency of the electrochemical oxidation process. Therefore, the main target of this paper is to simultaneously increase COD and TOC removal efficiencies using artificial intelligence and modern optimization. Firstly, an accurate model based on ANFIS was established to simulate the electrochemical oxidation process in terms of reaction time, pH, salt concentration, and DC applied voltage. Compared with ANOVA, thanks to ANFIS modelling, the RMSE values are decreased by 84% and 86%, respectively, for COD and TOC models. Additionally, the coefficient of determination values increased by 3.26% and 7.87% for COD and TOC models, respectively. Secondly, the optimal reaction time values, pH, salt concentration, and applied voltage were determined using the hunger games search algorithm (HGSA). To prove the effectiveness of the HGSA, a comparison with a slime mold algorithm, sine cosine algorithm, and Harris's hawks optimization was conducted. The optimal values were found at a pH of 8, a reaction time of 36.6 min, a salt concentration of 29.7 g/L, and a DC applied voltage of 9 V. Under this condition, the maximum COD and TOC removal values were 97.6% and 69.4%, respectively. The overall efficiency increased from 76.75% to 83.5% (increased by 6.75%).

Keywords: artificial intelligence; ANFIS modeling; environmental sciences; hunger games search; wastewater treatment



Citation: Rezk, H.; Olabi, A.G.; Sayed, E.T.; Alshathri, S.I.; Abdelkareem, M.A. Optimized Artificial Intelligent Model to Boost the Efficiency of Saline Wastewater Treatment Based on Hunger Games Search Algorithm and ANFIS. *Sustainability* **2023**, *15*, 4413. <https://doi.org/10.3390/su15054413>

Academic Editor:
Ioannis Katsoyiannis

Received: 17 December 2022
Revised: 28 January 2023
Accepted: 14 February 2023
Published: 1 March 2023



Copyright: © 2023 by the authors. Licensee MDPI, Basel, Switzerland. This article is an open access article distributed under the terms and conditions of the Creative Commons Attribution (CC BY) license (<https://creativecommons.org/licenses/by/4.0/>).

1. Introduction

Water and energy are two intertwined global issues. Access to safe drinking water is a major issue that affects a large number of people and is expected to worsen as a result of population growth. Water desalination is considered the best choice to secure sustainable fresh water; however, it requires a significant amount of energy [1]. Wastewater discharge has been on the rise in tandem with global population growth, industrialization, and urbanization [2–5]. While securing fresh water is critical for several countries, wastewater is discharged in large quantities. The proper treatment of such wastewater can secure a considerable portion of fresh water requirements. High salts can be found in various industrial wastewaters, including textiles, medicines, leather goods, fish, meat processing, and marine products [6,7]. Along with contaminated groundwater and wastewater from

mining operations and recycling units in the gas and oil industries, salt can also be discovered in significant amounts in the leachate of urban dumpsites [8,9]. The fish processing industry needs a lot of sodium chloride for preservation [10,11]. High salt concentrations are necessary in the tanning process used by the leather industry to strip hair and wool from animal skins [12,13]. Furthermore, the salt content of the effluent from the oil refining, extraction, and processing sectors varies significantly, often being several times higher than the salt content of saltwater [14].

If wastewater is not handled correctly, the environment and human health can suffer [15]. These consequences may involve harm to fish and wildlife populations, in addition to oxygen reduction and drinking water pollution [16]. The main purpose of wastewater treatment is the removal of suspended solids and metal ions before returning the effluent to the environment [17,18]. As solid organic matter decays, it consumes oxygen that is necessary for plants and animals. The proper treatment/management of wastewater signifies a genuine sanitary and environmental challenge for all stakeholders worldwide [19–24]. Effective treatment options are available, including reusing treated wastewater [25,26].

The biological wastewater treatment approach, the conventional wastewater treatment method, is a widespread treatment method [27,28]. It considers biodegradation bleaching with the help of various microorganisms, algae, yeast, fungi, and bacteria [29]. This simple and inexpensive process combines aerobic and anaerobic processes [30]. The use of biological treatment methods for treating saline wastewater is currently unattainable because of the dehydration of microbial cells in high-salt wastewater. Therefore, in the case of saline wastewater, salt removal is necessary before biological treatment [31]. However, conventional technologies rarely succeed in removing salt from wastewater. For the treatment of wastewater with a high salt concentration, membrane treatment methods, including reverse osmosis, nanofiltration, ultrafiltration–nanofiltration, and sophisticated oxidation processes, including electrolysis and the electro-Fenton process, have been proposed [32–34]. These wastewaters have a high electrical conductivity because of their high concentration of cations and anions. Therefore, treating such wastewater with electron-assisted approaches may be a good solution [35,36].

The reaction time, pH, salt concentration, and DC applied voltage are considered essential factors that influence the performance of the electrochemical oxidation process. The performance of the electrochemical oxidation process is measured through the chemical oxygen demand (COD) and total organic carbon (TOC) removal. Optimizing the controlling parameters, i.e., reaction time, pH, salt concentration, and the applied voltage, is essential to increase the overall performance of the treatment process in terms of COD and TOC removal efficiencies. Experimental optimization of such parameters is time-consuming, costly, and needs significant effort and money. Although there has been success in this regard using mathematical and physical modelling, the accuracy of these models is limited by the need for assumptions [37]. Artificial intelligence (AI) is a robust modelling and optimization method that is effectively used in various processes [38]. AI was applied successfully to modelling and optimizing the performance of microbial fuel cells in terms of increasing the power production at higher COD removal [22,39], biodiesel production [40,41], syngas production [42–44], biohydrogen production [45,46], power output of solid oxide fuel cells [47,48], carbon capture [49,50], and wastewater treatment [51]. Consequently, this work aims to improve the performance of the electrochemical oxidation process by simultaneously boosting the COD and TOC removal efficiencies using artificial intelligence and modern optimization. Unlike normal mathematical tools, ANFIS expresses the functionality between the output and the inputs in the form of some IF-THEN fuzzy rules. The proposed methodology for the case under investigation contains two phases. The first phase is building an accurate model using ANFIS to simulate the electrochemical oxidation process in terms of three controlling input parameters. The second phase is the optimal parameter identification process using the hunger games search algorithm (HGSA). During the optimization process, three controlling parameters were used. The reaction time, pH, salt concentration, and DC applied voltage were used as decision variables, whereas

the objective function was simultaneously maximization of the COD and TOC removal efficiencies.

The main contributions can be outlined as follows.

- Creating an precise ANFIS model of the electrochemical oxidation process.
- For the first time, a hunger games search algorithm is used to define the best values of reaction time, pH, salt concentration, and DC applied voltage
- Boosting the COD and TOC removal efficiencies simultaneously
- Demonstration of the proposed methodology

2. Materials, Methods, and Dataset

A rectangular Plexiglas reactor with a dimension of $15 \times 6 \times 16$ and 1 L working volume operated under batch mode was used. Two parallel electrode series of iron with a dimension of 1.6 cm diameter and 14 cm length were connected and put inside the Plexiglas reactor and contacted with the power supply as seen in Figure 1. Synthetic saline wastewater with total organic carbon and chemical oxygen demand (COD) concentrations of 2000 mg/L and 3500 mg/L, respectively, was synthesized by adding sodium chloride (to control salinity) to wastewater. The pH of the synthetic saline wastewater was adjusted using 1 N HCl and NaOH. COD and TOC were measured according to the standard methods reported in [52]. The process's efficiency was assessed based on COD and TOC removal efficiencies according to the following equation:

$$\text{TOC or COD removal efficiency \%} = \frac{C_i - C}{C_i} \times 100$$

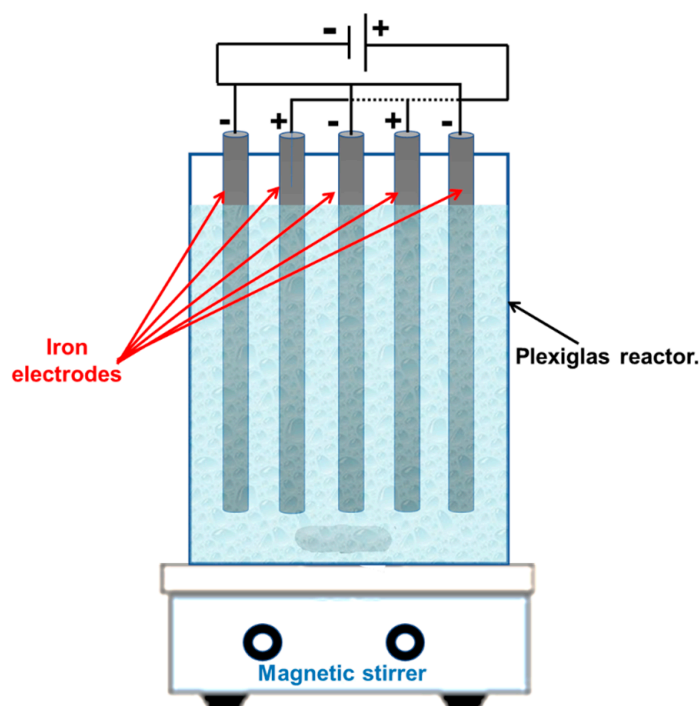


Figure 1. Scheme of the electro-oxidation Plexiglas reactor.

C_i is the initial concentration in mg/L (TOC or COD), and C is the final concentration in mg/L (TOC or COD). The influence of reaction time, pH, applied voltage, and salt concentration on the TOC and COD removal efficiency was investigated. The values of these independent values were shown in Table 1. The experimental results obtained are shown in Table 2:

Table 1. Considered parameters.

Independent Variables	Values
Reaction time, min	20, 30, 40
pH	4, 6, 8
Applied voltage, V	3, 6, 9
Salt concentration, mg/L	12,000, 22,000, 32,000

Table 2. Effect of different operating parameters on COD and TOC [36], open access.

pH	Time (min)	Salinity (gr/L)	Voltage (Volt)	COD Removal (%)	TOC Removal (%)
4	20	22	6	49	37
4	30	22	3	38	36
4	30	12	6	49	37
4	30	22	9	69	55
4	30	32	9	51	40
4	40	22	6	60	37
6	20	12	6	36	30
6	20	22	3	51	30
6	20	22	9	43	40
6	20	32	6	57	32
6	30	12	3	43	39
6	30	12	9	52	40
6	30	22	6	80	67
6	30	22	6	79.4	61.7
6	30	22	6	86	66
6	30	22	6	83	62
6	30	22	6	81	67
6	30	32	3	51	37
6	30	32	9	81	62
6	40	12	6	52	37
6	40	22	3	53	31
6	40	22	9	83	60
6	40	32	6	73	54
8	30	12	6	57.5	42
8	30	22	3	71	52
8	30	22	9	81.5	58.2
8	30	32	6	89	64.5
8	40	22	6	76	44

3. Methodology

The considered methodology comprises two stages: ANFIS modelling and optimal parameter determination.

3.1. ANFIS-Modelling

For the ANFIS model, the nonlinear mapping of the inputs is achieved using membership functions (MFs) during the fuzzification stage. Creating the rules, evaluating the rules' outputs, and merging the fired rules to obtain the output occurs during the inference engine phase [53]. Ultimately, the output is switched from a fuzzy shape to a crisp shape during the defuzzification stage. Despite various MF shapes and defuzzification methods, the Gaussian structure and weight average are considered in this work. The relationships between the inputs and outputs are patterned by an IF-THEN system as presented as follows [49]:

IF x is X and y is Y THEN $z = f(x, y)$;

Where, x and y represent the inputs and z denotes the output; X and Y denote the membership functions.

The output f is defined in terms of the two rules' outputs, f_1 and f_2 , as follows:

$$\begin{array}{ll}
 f = \tilde{\omega}_1 f_1 + \tilde{\omega}_2 f_2 & \text{(Output Layer)} \\
 \text{Evaluating } \tilde{\omega}_1 g_1(x, y) \text{ and } \tilde{\omega}_2 g_2(x, y) & \text{(Defuzzification Layer)} \\
 \tilde{\omega}_1 = \frac{\omega_1}{\omega_1 + \omega_2} \text{ and } \tilde{\omega}_2 = \frac{\omega_2}{\omega_1 + \omega_2} & \text{(N Layer)} \\
 \omega_1 = \mu_{A_1} * \mu_{B_1} \text{ and } \omega_2 = \mu_{A_2} * \mu_{B_2} & \text{(\pi Layer)} \\
 \mu_{A_1}, \mu_{A_2}, \mu_{B_1} \text{ and } \mu_{B_2} \text{ are the MF values of the two inputs} & \text{(Fuzzification Layer)}
 \end{array}$$

3.2. Hunger Games Search

The original code of HGS is proposed by Yang et al. [54]. We integrated this optimizer for the first time with ANFIS modelling to determine the best values of the reaction time, pH, salt concentration, and DC applied voltage in order to improve the efficiency of the electrochemical oxidation process. The behavior of the HGS can be expressed mathematically to emulate the contraction stage as follows [54]:

$$X(t+1) = \begin{cases} \vec{X}(t) \cdot (1 + \text{randn}(1)), & r_1 < l \\ \vec{W}_1 \cdot \vec{X}_b + \vec{R} \cdot \vec{W}_2 \cdot \left| \vec{X}_b - \vec{X}(t) \right|, & r_1 > l, r_2 > E \\ \vec{W}_1 \cdot \vec{X}_b - \vec{R} \cdot \vec{W}_2 \cdot \left| \vec{X}_b - \vec{X}(t) \right|, & r_1 > l, r_2 < E \end{cases} \quad (1)$$

where r_1 and r_2 are randoms;

t is current iterations;

\vec{W}_1 and \vec{W}_2 are the weights of hunger;

\vec{X}_b is the location information of a random individual in all the optimal individuals;

$\vec{X}(t)$ is each individual's location;

The expression of E is presented in (2) [54].

$$E = \text{sech}(|F(i) - BF|) \quad (2)$$

where $i \in 1, 2, \dots, n$, $F(i)$ is the fitness value;

BF denotes the best fitness;

Sech denotes a hyperbolic function $\left(\text{sech}(x) = \frac{2}{e^x + e^{-x}} \right)$.

The expression of \vec{R} is presented in (3):

$$\vec{R} = 2 \times a \times \text{rand} - a \quad (3)$$

$$a = 2 \times \left(1 - \frac{t}{\text{Max_iter}} \right) \quad (4)$$

where rand denotes a random value;

Max_iter denotes the maximum iterations number.

The starvation characteristics of particles can be presented as follows:

The expressions of \vec{W}_1 and \vec{W}_2 can be presented as in (5) and (6) respectively [54]:

$$\vec{W}_1(i) = \begin{cases} \text{hungry}(i) \cdot \frac{N}{SHungry} \times r_4, & r_3 < l \\ 1, & r_3 > l \end{cases} \quad (5)$$

$$\vec{W}_2(i) = (1 - \exp(-|\text{hungry}(i) - SHungry|)) \times r_5 \times 2 \quad (6)$$

here hungry denotes the hunger of every particle;

N is the number of particles;

$SHungry$ is the sum of hungry feelings of all particles;

r_3 , r_4 and r_5 denote randoms values.

The expression for $hungry(i)$ can be presented as follows:

$$hungry(i) = \begin{cases} 0, & AllFitness(i) == BF \\ hungry(i) + H, & AllFitness(i) \neq BF \end{cases} \quad (7)$$

where $AllFitness(i)$ is the fitness of every particle in the present iteration.

The expression for H is presented in (9):

$$TH = \frac{F(i) - BF}{WF - BF} \times r_6 \times 2 \times (UB - LB) \quad (8)$$

$$H = \begin{cases} LH \times (1 + r), & TH < LH \\ TH, & TH \geq LH \end{cases} \quad (9)$$

where r_6 is a random value;

$F(i)$ is the fitness of every particle;

BF denotes the best fitness;

WF is the worst fitness obtained in the current iteration process;

UB and LB are the maximum and minimum limits;

The hunger sensation H is limited to a lower bound, LH .

4. Results and Discussion

The number of measured points that were used for creating the ANFIS model is 29. These samples were distributed to two parties. The first part had 20 samples. It was employed to train the model, whereas the reminder was employed to test it. The ANFIS model was trained by LSE and backpropagation in the forward and backward paths, respectively. The SC was adopted for generation ANFIS rules. In this work the number of rules are 17 and 19 for COD and TOC models, respectively. Next, the models were trained until the minimum RMSE value was attained. The statistical assessment of the ANFIS-based model is explained in Table 3.

Table 3. Statistical assessment of ANFIS-based models of COD and TOC.

RMSE			R-Squared		
Train	Test	All	Train	Test	All
COD model					
0.611	6.74	3.79	0.999	0.91	0.95
TOC model					
0.838	4.547	2.63	0.994	0.92	0.96

Referring to Table 1, the RMSE values were 0.611 and 6.74 during training and testing, respectively, of the COD-based model. The R -squared values were 0.999 and 0.91 during training and testing the model, respectively. The RMSE decreased from 23.7 using ANOVA [36] to 3.79 using ANFIS (decrease of 84%). The adjusted R -squared increased from 0.92 using ANOVA to 0.95 using ANFIS (increase of 3.26%). For the TOC-based ANFIS model, the RMSE values were 0.838 and 4.547 for training and testing data, respectively. The R -squared values were 0.994 and 0.92 for training and testing. Compared with ANOVA [36], the RMSE decreased from 18.78 using ANOVA to 2.63 using ANFIS (decrease of 86%). The adjusted R -squared raised from 0.89 using ANOVA to 0.96 using ANFIS (increase of 7.87%). In sum, the lowered RMSE and the boosted R -squared values of the ANFIS model demonstrate a successful modelling stage. Figure 2a,b presents the 4-inputs-single-output structure of the ANFIS model for COD and TOC. There were 17 and 19 rules for COD and TOC models, respectively. To obtain the rules, the subtractive clustering method was used. The shapes of the Gaussian MFs are presented in Figure 3a,b for COD and TOC models. The colors in Figure 3 represent the clusters.

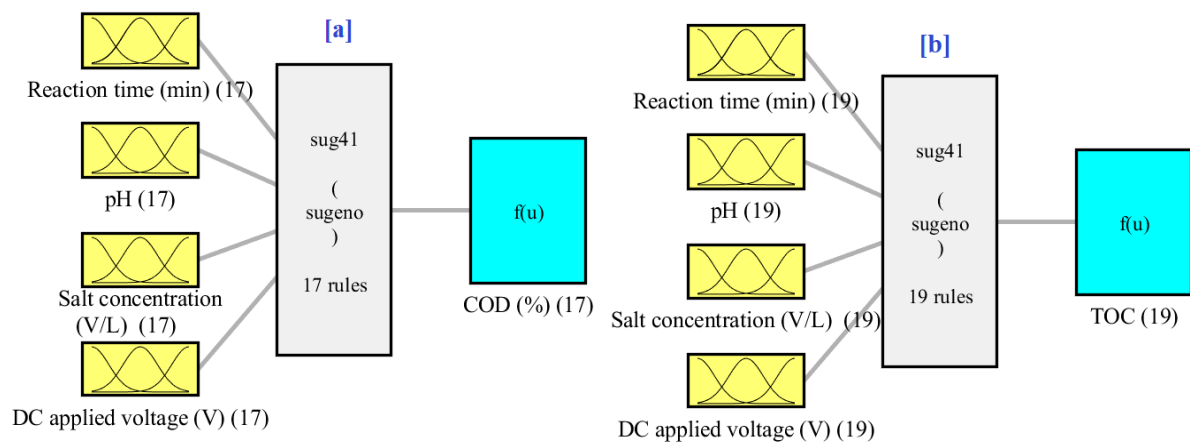


Figure 2. Arrangement of ANFIS models; (a) COD and (b) TOC.

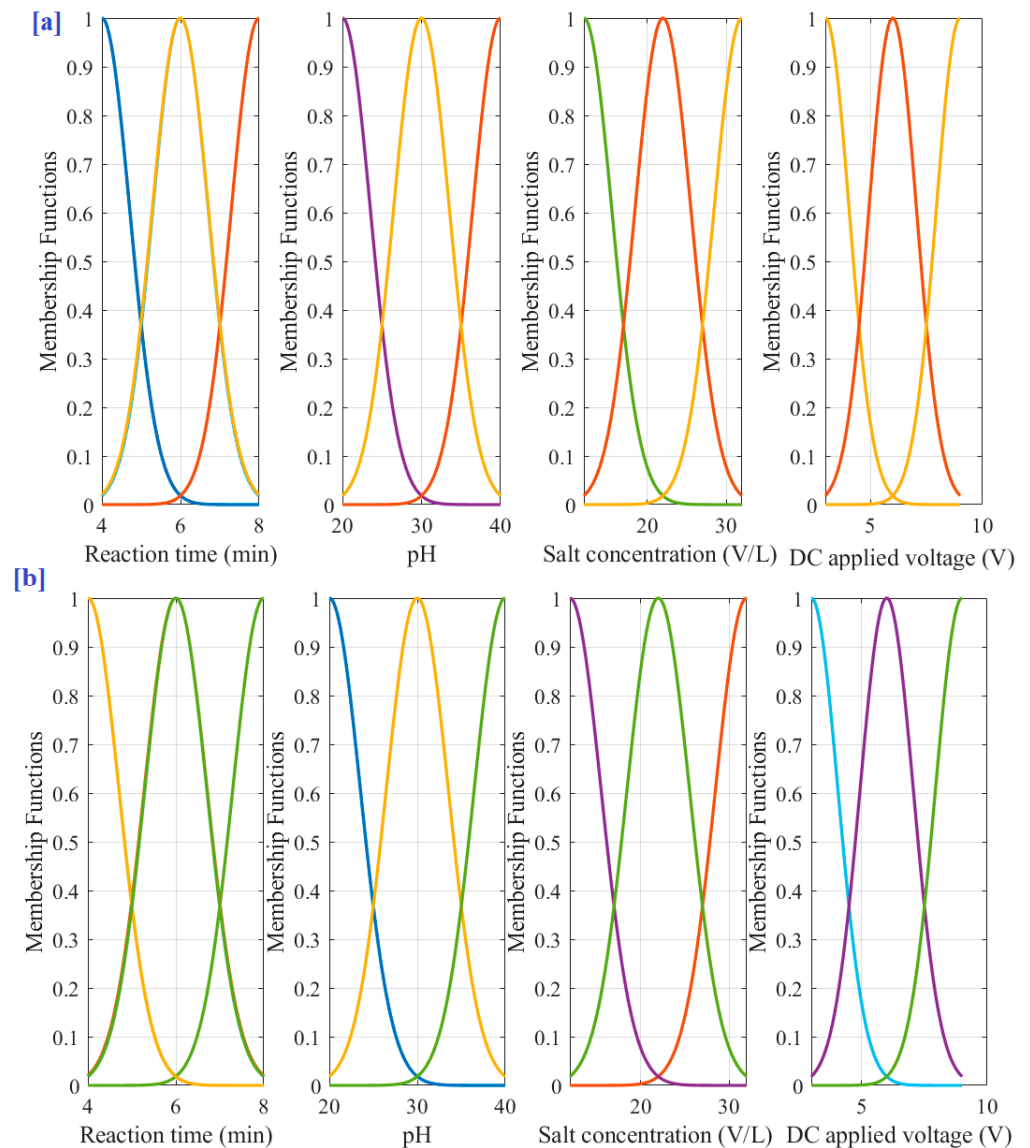


Figure 3. Input MFs of ANFIS models; (a) COD and (b) TOC.

Figures 4 and 5 point out the three-dimensional description with contours of the system's input–output for COD and TOC models, respectively. The maximum point of the output reaches dark red, but the minimum point reaches dark blue.

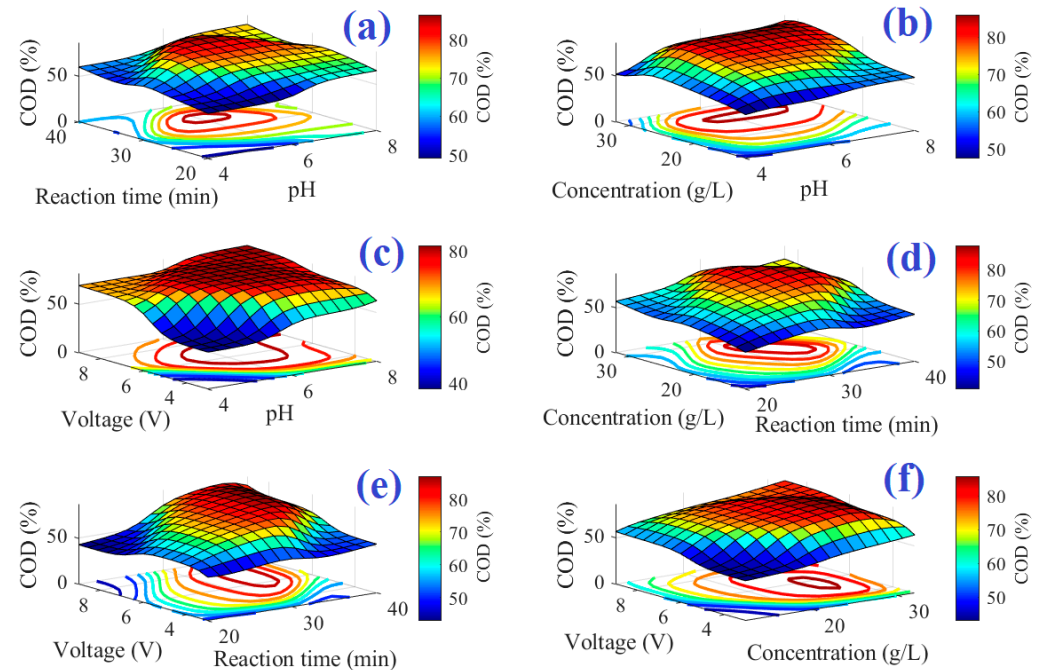


Figure 4. The surface of ANFIS-based models for COD removal at the different interactions of (a) pH and reaction time, (b) pH and salt concentration, (c) applied voltage and pH, (d) salt concentration and reaction time, (e) applied voltage and reaction time, and (f) applied voltage and salt concentration.

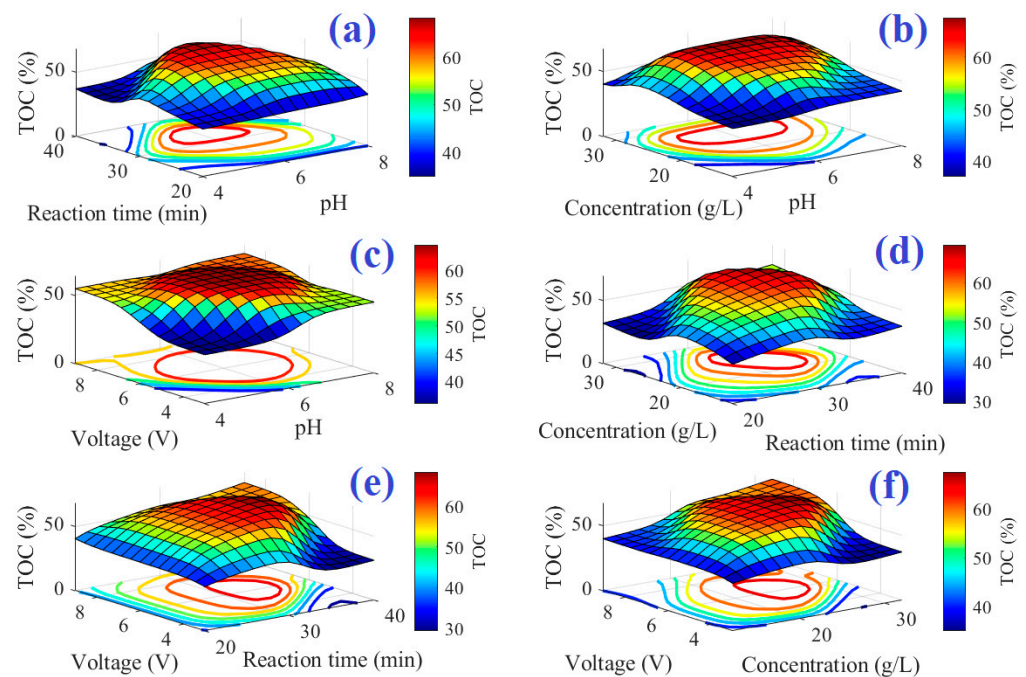
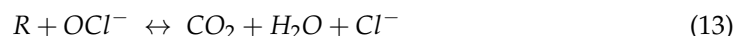


Figure 5. The surface of ANFIS-based models for TOC at the different interactions of (a) pH and reaction time, (b) pH and salt concentration, (c) applied voltage and pH, (d) salt concentration and reaction time, (e) applied voltage and reaction time, and (f) applied voltage and salt concentration.

Figure 4 illustrates the surface of ANFIS-based models for COD removal at the different interactions of (a) pH and reaction time, (b) pH and salt concentration, (c) applied voltage and pH, (d) salt concentration and reaction time, (e) applied voltage and reaction time, and (f) applied voltage and salt concentration. As depicted in the figure, there is an optimum condition of the various parameters, i.e., pH, salt concentration, reaction time, and applied voltage. As shown in these figures, as the salt concentration increases, so does the percentage of COD and TOC removed. This is due to indirect oxidation caused by the production of chloride or hypochlorite in response to the NaCl electrolysis process occurring in the reactor, which, together with the produced hydroxyl radicals, causes organic compound degradation [55]. The values of COD and TOC removal increase as pH values rise. This rising trend is predicted for pH values up to 7, after which the removal percentage will continue to fall. Chloride compounds such as hypochlorite, chloride ions, chlorine gas, and chlorate are formed during electrochemical treatment. The appropriate pH for this study was alkaline. The chlorine gas produced from Cl⁻ ions at the anode (Equation (10)) is converted to hydrolyzed hypochlorite in this alkaline environment via the following reactions (Equations (11) and (12)) [36]:



Such hypochlorite ions are used in the oxidation of the organic materials according to the following equation (Equation (13)):



As is clear from the figure, the TOC and COD removal increased over time until 30 min, and then decreased with a further increase in time. The optimum time for the COD and TOC removal was around 30 min. This is because as reaction time increases, the percentage removal of the TOC and COD increases, however, as time proceeds, the salt concentration (responsible for the hypochlorite production) decreases, and thus the percentage removal decreases again. Furthermore, it is clear that the increase in the applied voltage from 4 to 6 V increased the removal percentages of the TOC and COD. However, they decreased at higher applied voltages. This could be related to the sequestration of metal hydroxides at the electrode level [36,56]. The increase in the salt concentration resulted in an increase in both TOC and COD removal, and again they decreased at higher salt concentrations beyond 22 g/L. The increased removal percentages with increasing salt concentration could be related to the positive role of the Cl on the oxidation of the organic materials, as discussed above and reported by Panizza and Cerisola [57]. However, at higher salt concentrations, the evolution of the Cl₂ gas from the reactor decreased the removal percentages.

Catching the accurate relation between the inputs and outputs of electrochemical oxidation motivates the created model to estimate both COD and TOC perfectly. This is obvious from the mapping of the ANFIS model's predicted outputs with the measured dataset as illustrated in Figure 6a–d, for training the COD model, training the TOC model, testing the COD model, and testing the TOC model, respectively. There is a match between both experimental and ANFIS data. In addition, the predictions' plots across the 100% accuracy line are demonstrated in Figure 7a,b, respectively, for COD and TOC during the training period.

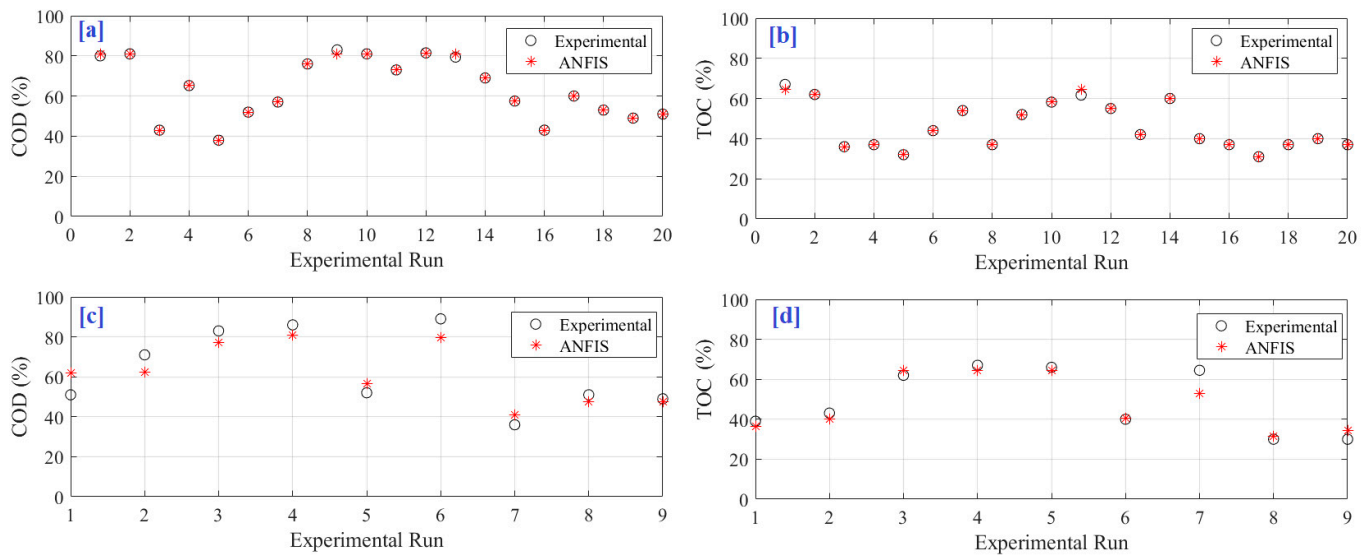


Figure 6. Predicted versus experimental data of fuzzy model. (a) Training COD model, (b) Training TOC model, (c) Testing COD model and (d) Testing TOC model.

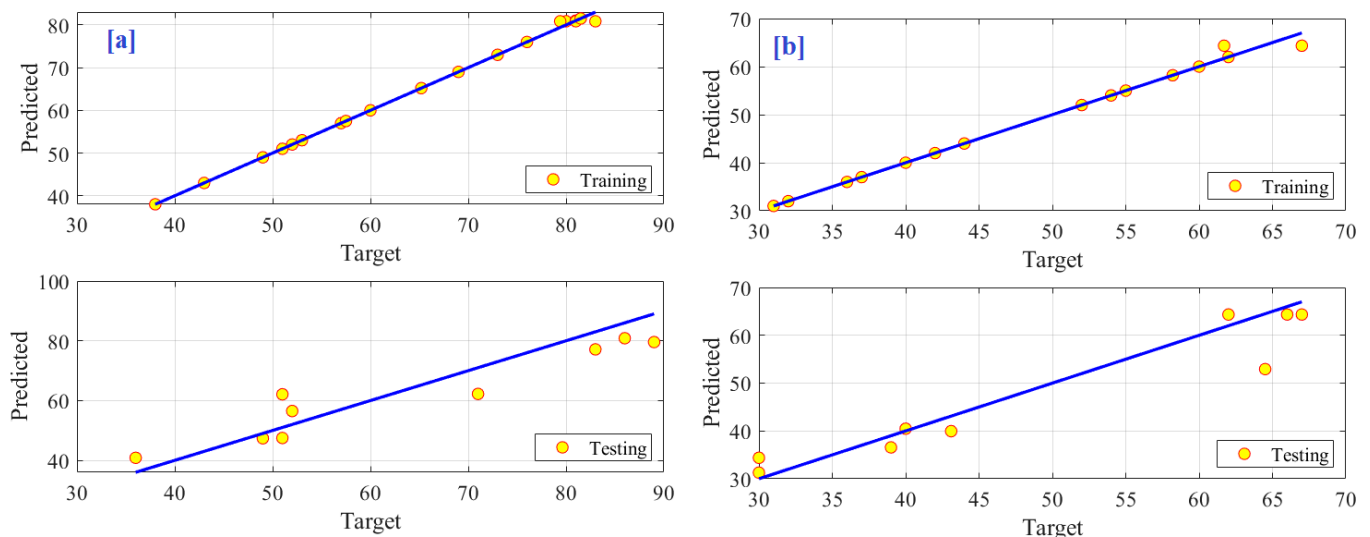


Figure 7. Prediction accuracy of ANFIS-based models. (a) COD and (b) TOC.

The following section shows the parameter identification process. The parameter identification process aims to define the optimal values of reaction time, pH, salt concentration, and applied voltage to increase COD and TOC simultaneously. Consequently, after creating a consistent ANFIS model, HGSA was used to define the optimal values for four input parameters. To prove the effectiveness of HGSA, a comparison was made with slime mold algorithm, sine cosine algorithm (SCA) and Harris's hawks optimization (HHO). The following relation can define the optimization problem of the case study:

$$f = \operatorname{argmax}_{x \in R} (COD + TOC)$$

where x is the four input parameters.

Table 4 presents the optimal values of action time, pH, salt concentration, and DC applied voltage and the corresponding COD and TOC using measured data, RSM methodology, and the HGSA. The combination between ANFIS and HGSA simultaneously increased the COD and TOC. The COD increased to 97.63% with a rate of 9.7% and 6.4% compared to

experimental and RSM methodology, respectively. In the same way, the TOD increased to 69.42% with a rate of 7.63% and 1.4% compared with measured data and RSM methodology, respectively.

Table 4. Optimal values of input controlling parameters.

Method	Reaction Time	pH	Salt Concentration (g/L)	DC Applied Voltage	COD (%)	TOC (%)
Exp. [36]	30	8	32	6	89	64.5
RSM [36]	30.71	7.69	30.94	7.41	91.78	68.49
HGSA	36.69	8	29.9	9.0	97.63	69.42

To check the robustness of the considered optimization algorithms, each one was implemented 30 times. Table 5 demonstrates a comparison among the considered algorithms. The number of populations (5) and iterations (100) were fixed with algorithms during the optimization. Table 5 shows the superiority of HGSA compared with SMA, SCA, and HHO. HGSA achieved the lowest STD value of 0.0127, whereas the maximum STD of 3.2264 was obtained by HHO. Figure 8 demonstrates the statistical analysis of 30 runs. Figure 8a shows the maximum objective function found over 30 runs of HGSA. The details of the 30 run values for HGSA, HHO, SCA, and SMA are presented in Figure 8b–e. The best mean cost function of 166.9904 was obtained by HGSA, whereas SCA obtained the worst cost of 155.2735. This demonstrated the efficacy of the suggested methodology. Figure 9a–d shows the particle convergence during the optimization process for reaction time, pH, salt concentration, and DC applied voltage, respectively. As presented in Figure 8, the optimal solutions were 36.69 min, 8, 29.9 g/L, and 9.0 V, respectively, for reaction time, pH, salt concentration, and DC applied voltage.

Table 5. Comparison between considered algorithms.

	HGSA	SMA	SCA	HHO
Maximum	167.0600	167.0600	166.8933	167.0442
Minimum	166.9904	158.1047	155.2735	156.5687
Mean	167.0577	165.8614	163.0845	165.0988
STD	0.0127	3.0856	3.1572	3.2264

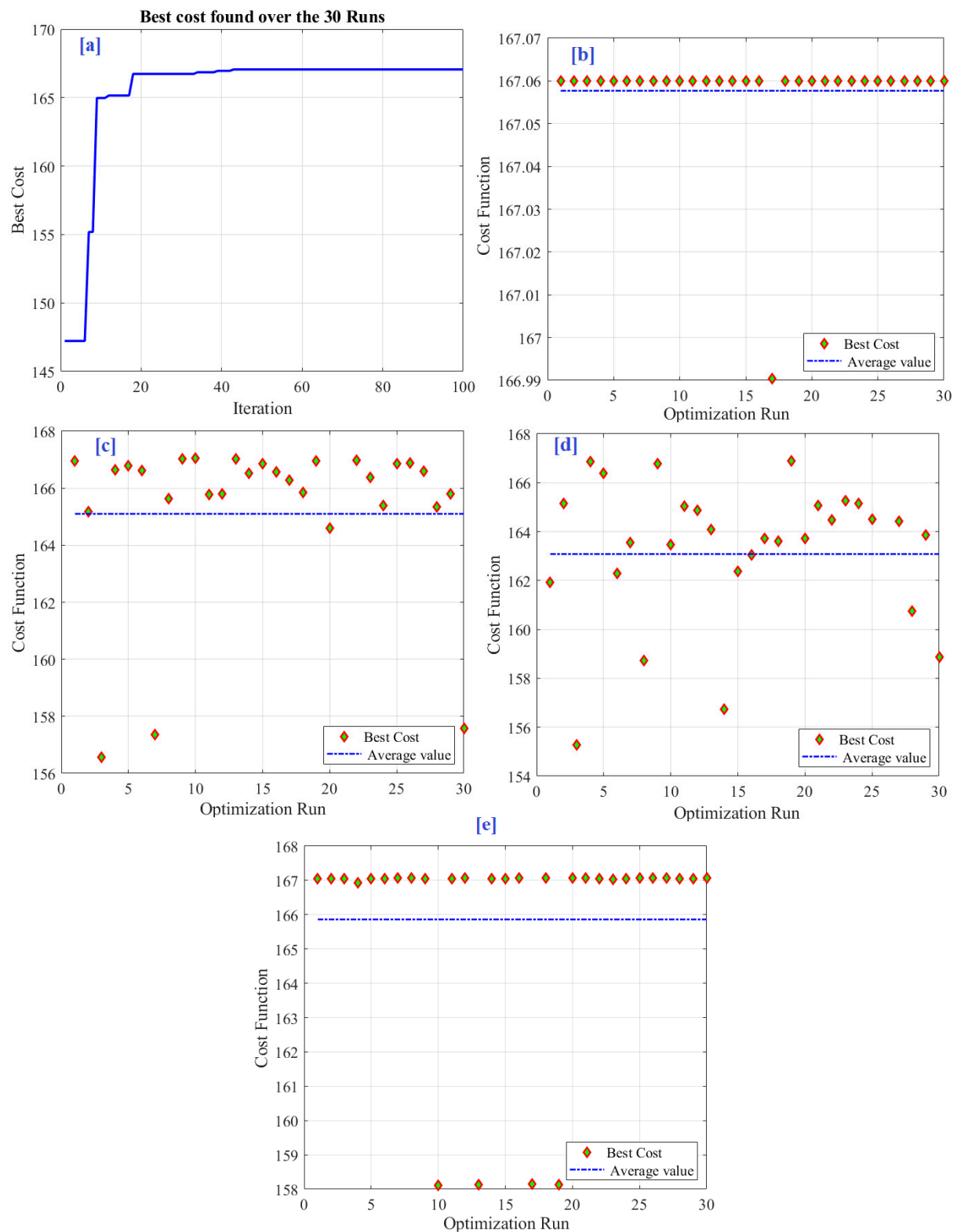


Figure 8. Optimized results (a) maximum objective function found over 30 run of HGSA, (b) HGSA, (c) HHO, (d) SCA and (e) SMA.

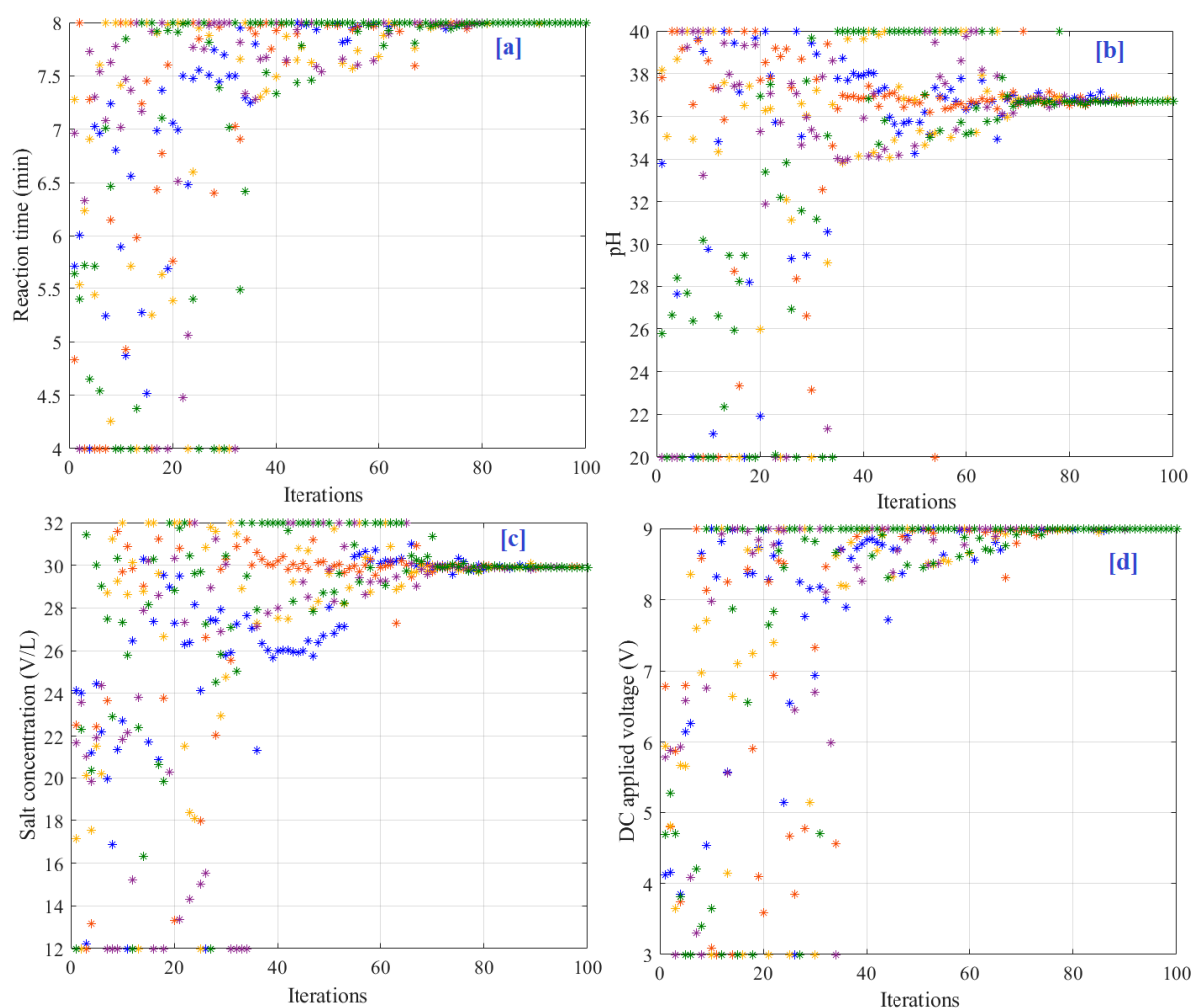


Figure 9. Particle convergence during optimization process. (a) reaction time, (b) pH, (c) Salt concentration and (d) DC applied voltage.

5. Conclusions

The objective of this research is to model and optimize the performance of the electrochemical oxidation process. The methodology integrates the ANFIS modelling and parameter identification with HGSA. Two important outputs, COD and TOC removal efficiencies of saline wastewater treatment, were increased through optimal tuning of the reaction time, pH, salt concentration, and DC applied voltage. The ANFIS model was compared with ANOVA. At first, a robust ANFIS-based model of the electrochemical oxidation process was created. Compared with ANOVA, the COD-based ANFIS model's RMSE value was reduced from 23.7 using ANOVA to 3.79 using ANFIS. This is a decrease of 84%. The adjusted *R*-squared was boosted from 0.92 (ANOVA) to 0.95 (ANFIS). This is an increase of 3.26%. Additionally, for the TOC-based ANFIS model, the RMSE value was reduced from 18.78 using ANOVA to 2.63 using ANFIS. This is a decrease of 86%. The adjusted *R*-squared was boosted from 0.89 (ANOVA) to 0.96 (ANFIS). This is an increase of 7.87%. This proved the accuracy of ANFIS modelling. Then, using HGSA, the best values for controlling parameters of 36.69 min, 8, 29.9 g/L and 9.0 V were identified for reaction time, pH, salt concentration, and DC applied voltage, respectively. Under this condition, the COD increased to 97.63% with a rate of 9.7% and 6.4% compared with measured data and RSM methodology, respectively. In the same direction, the TOD increased to 69.42% with a rate of 7.63% and 1.4% compared with measured data and RSM methodology, respectively.

Author Contributions: Conceptualization, A.G.O., H.R. and M.A.A.; methodology H.R., E.T.S. and S.I.A.; formal analysis, E.T.S. and S.I.A.; investigation, S.I.A. and M.A.A.; resources, A.G.O. and S.I.A.; data curation, E.T.S.; writing—original draft preparation, A.G.O., H.R., E.T.S., S.I.A. and M.A.A.; writing—review and editing, A.G.O., H.R., E.T.S., S.I.A. and M.A.A.; supervision, A.G.O. and M.A.A.; project administration, H.R. and E.T.S. All authors have read and agreed to the published version of the manuscript.

Funding: This research was funded by Princess Nourah bint Abdulrahman University Researchers Supporting Project number (PNURSP2023R197), Princess Nourah bint Abdulrahman University, Riyadh, Saudi Arabia.

Institutional Review Board Statement: Not applicable.

Informed Consent Statement: Not applicable.

Data Availability Statement: Not applicable.

Acknowledgments: Princess Nourah bint Abdulrahman University Researchers Supporting Project number (PNURSP2023R197), Princess Nourah bint Abdulrahman University, Riyadh, Saudi Arabia.

Conflicts of Interest: The authors declare no conflict of interest.

References

1. Sayed, E.T.; Olabi, A.G.; Elsaid, K.; Al Radi, M.; Alqadi, R.; Ali Abdelkareem, M. Recent progress in renewable energy based-desalination in the Middle East and North Africa MENA region. *J. Adv. Res.* **2022**. [\[CrossRef\]](#)
2. Yu, Y.; Wu, B.; Jiang, L.; Zhang, X.-X.; Ren, H.-Q.; Li, M. Comparative analysis of toxicity reduction of wastewater in twelve industrial park wastewater treatment plants based on battery of toxicity assays. *Sci. Rep.* **2019**, *9*, 3751. [\[CrossRef\]](#) [\[PubMed\]](#)
3. Heydari Orojloo, S.; Rastegarzadeh, S.; Zargar, B. Experimental and modeling analyses of COD removal from industrial wastewater using the TiO₂-chitosan nanocomposites. *Sci. Rep.* **2022**, *12*, 11088. [\[CrossRef\]](#) [\[PubMed\]](#)
4. Ali, N.S.; Kalash, K.R.; Ahmed, A.N.; Albayati, T.M. Performance of a solar photocatalysis reactor as pretreatment for wastewater via UV, UV/TiO₂, and UV/H₂O₂ to control membrane fouling. *Sci. Rep.* **2022**, *12*, 16782. [\[CrossRef\]](#) [\[PubMed\]](#)
5. Charazińska, S.; Burszta-Adamiak, E.; Lochyński, P. The efficiency of removing heavy metal ions from industrial electropolishing wastewater using natural materials. *Sci. Rep.* **2022**, *12*, 17766. [\[CrossRef\]](#)
6. Zhou, G.; Wang, X.; Zhao, H.; Zhang, W.; Liu, G.; Zhang, X. Isolation of two salt-tolerant strains from activated sludge and its COD degradation characteristics from saline organic wastewater. *Sci. Rep.* **2020**, *10*, 18421. [\[CrossRef\]](#)
7. Cui, Y.-W.; Zhang, H.-Y.; Ding, J.-R.; Peng, Y.-Z. The effects of salinity on nitrification using halophilic nitrifiers in a Sequencing Batch Reactor treating hypersaline wastewater. *Sci. Rep.* **2016**, *6*, 24825. [\[CrossRef\]](#)
8. Chandnani, G.; Gandhi, P.; Kanpariya, D.; Parikh, D.; Shah, M. A comprehensive analysis of contaminated groundwater: Special emphasis on nature-ecosystem and socio-economic impacts. *Groundw. Sustain. Dev.* **2022**, *19*, 100813. [\[CrossRef\]](#)
9. Awuchi, C.G.; Hannington, T.; Awuchi, C.G.; Igwe, V.S.; Amagwula, I.O. Industrial waste management, treatment, and health issues: Wastewater, solid, and electronic wastes. *Eur. Acad. Res.* **2020**, *8*, 1081–1119.
10. Aheto, J.H.; Huang, X.; Xiaoyu, T.; Bonah, E.; Ren, Y.; Alenyorege, E.A.; Chunxia, D. Investigation into crystal size effect on sodium chloride uptake and water activity of pork meat using hyperspectral imaging. *J. Food Process. Preserv.* **2019**, *43*, e14197. [\[CrossRef\]](#)
11. Kanagaraj, J.; Panda, R.C.; Kumar, V. Trends and advancements in sustainable leather processing: Future directions and challenges—A review. *J. Environ. Chem. Eng.* **2020**, *8*, 104379.
12. Dowlath, M.J.H.; Karuppanan, S.K.; Rajan, P.; Khalith, S.M.; Rajadesingu, S.; Arunachalam, K.D. Application of advanced technologies in managing wastes produced by leather industries—An approach toward zero waste technology. In *Concepts of Advanced Zero Waste Tools*; Elsevier: Amsterdam, The Netherlands, 2021; pp. 143–179.
13. Venkatachalam, M.; Rathinam, A.; Rao, J.; Krishnan, C. Bioconversion of animal hair waste using salt- and sulphide-tolerant *Bacillus* sp. KLP1 and depilation using keratinase. *Int. J. Environ. Sci. Technol.* **2022**, *19*, 6389–6398. [\[CrossRef\]](#)
14. Das, B.; Deka, S. A cost-effective and environmentally sustainable process for phycoremediation of oil field formation water for its safe disposal and reuse. *Sci. Rep.* **2019**, *9*, 15232. [\[CrossRef\]](#) [\[PubMed\]](#)
15. Shaikh, S.S.; Abu-Dieyeh, M.H.; Al Naemi, F.A.; Ahmed, T.; Al-Ghouti, M.A. Environmental impact of utilization of “produced water” from oil and gas operations in turfgrass systems. *Sci. Rep.* **2020**, *10*, 15051. [\[CrossRef\]](#) [\[PubMed\]](#)
16. Sun, W.; Xu, X.; Lv, Z.; Mao, H.; Wu, J. Environmental impact assessment of wastewater discharge with multi-pollutants from iron and steel industry. *J. Environ. Manag.* **2019**, *245*, 210–215. [\[CrossRef\]](#)
17. Hasanpour, M.; Hatami, M. Photocatalytic performance of aerogels for organic dyes removal from wastewaters: Review study. *J. Mol. Liq.* **2020**, *309*, 113094. [\[CrossRef\]](#)
18. Hasanpour, M.; Hatami, M. Application of three dimensional porous aerogels as adsorbent for removal of heavy metal ions from water/wastewater: A review study. *Adv. Colloid Interface Sci.* **2020**, *284*, 102247. [\[CrossRef\]](#)

19. Wilberforce, T.; Sayed, E.T.; Abdelkareem, M.A.; Elsaied, K.; Olabi, A.G. Value added products from wastewater using bioelectrochemical systems: Current trends and perspectives. *J. Water Process Eng.* **2021**, *39*, 101737. [\[CrossRef\]](#)
20. Sayed, E.T.; Alawadhi, H.; Elsaied, K.; Olabi, A.G.; Adel Almakrani, M.; Bin Tamim, S.T.; Alafrangi, G.H.M.; Abdelkareem, M.A. A Carbon-Cloth Anode Electroplated with Iron Nanostructure for Microbial Fuel Cell Operated with Real Wastewater. *Sustainability* **2020**, *12*, 6538. [\[CrossRef\]](#)
21. Sayed, E.T.; Alawadhi, H.; Olabi, A.G.; Jamal, A.; Almahdi, M.S.; Khalid, J.; Abdelkareem, M.A. Electrophoretic deposition of graphene oxide on carbon brush as bioanode for microbial fuel cell operated with real wastewater. *Int. J. Hydrog. Energy* **2021**, *46*, 5975–5983. [\[CrossRef\]](#)
22. Rezk, H.; Olabi, A.G.; Abdelkareem, M.A.; Maghrabie, H.M.; Sayed, E.T. Fuzzy Modelling and Optimization of Yeast-MFC for Simultaneous Wastewater Treatment and Electrical Energy Production. *Sustainability* **2023**, *15*, 1878. [\[CrossRef\]](#)
23. Sayed, E.T.; Olabi, A.G.; Shehata, N.; Al Radi, M.; Majdy Muhaisen, O.; Rodriguez, C.; Ali Atieh, M.; Abdelkareem, M.A. Application of bio-based electrodes in emerging capacitive deionization technology for desalination and wastewater treatment. *Ain Shams Eng. J.* **2022**, 102030. [\[CrossRef\]](#)
24. Mohamed, H.O.; Obaideen, M.; Sayed, E.T.; Abdelkareem, M.A.; Park, M.; Liu, Y.; Kim, H.-Y.; Barakat, N.A.M. Graphite Sheets as High-Performance Low-Cost Anodes for Microbial Fuel Cells Using Real Food Wastewater. *Chem. Eng. Technol.* **2017**, *40*, 2243–2250. [\[CrossRef\]](#)
25. Phung, L.D.; Pham, D.V.; Sasaki, Y.; Masuda, S.; Takakai, F.; Kaku, N.; Watanabe, T. Continuous sub-irrigation with treated municipal wastewater for protein-rich rice production with reduced emissions of CH₄ and N₂O. *Sci. Rep.* **2020**, *10*, 5485. [\[CrossRef\]](#) [\[PubMed\]](#)
26. Salgot, M.; Folch, M. Wastewater treatment and water reuse. *Curr. Opin. Environ. Sci. Health* **2018**, *2*, 64–74. [\[CrossRef\]](#)
27. Zhu, T.-T.; Su, Z.-X.; Lai, W.-X.; Zhang, Y.-B.; Liu, Y.-W. Insights into the fate and removal of antibiotics and antibiotic resistance genes using biological wastewater treatment technology. *Sci. Total Environ.* **2021**, *776*, 145906. [\[CrossRef\]](#)
28. Obaideen, K.; Abdelkareem, M.A.; Wilberforce, T.; Elsaied, K.; Sayed, E.T.; Maghrabie, H.M.; Olabi, A.G. Biogas role in achievement of the sustainable development goals: Evaluation, Challenges, and Guidelines. *J. Taiwan Inst. Chem. Eng.* **2022**, *131*, 104207. [\[CrossRef\]](#)
29. Zhao, Y.; Liu, D.; Huang, W.; Yang, Y.; Ji, M.; Nghiem, L.D.; Trinh, Q.T.; Tran, N.H. Insights into biofilm carriers for biological wastewater treatment processes: Current state-of-the-art, challenges, and opportunities. *Bioresour. Technol.* **2019**, *288*, 121619. [\[CrossRef\]](#)
30. Aziz, A.; Basheer, F.; Sengar, A.; Khan, S.U.; Farooqi, I.H. Biological wastewater treatment (anaerobic-aerobic) technologies for safe discharge of treated slaughterhouse and meat processing wastewater. *Sci. Total Environ.* **2019**, *686*, 681–708. [\[CrossRef\]](#)
31. Ahmad, N.N.R.; Ang, W.L.; Leo, C.P.; Mohammad, A.W.; Hilal, N. Current advances in membrane technologies for saline wastewater treatment: A comprehensive review. *Desalination* **2021**, *517*, 115170. [\[CrossRef\]](#)
32. Goh, P.; Wong, K.; Ismail, A. Membrane technology: A versatile tool for saline wastewater treatment and resource recovery. *Desalination* **2022**, *521*, 115377. [\[CrossRef\]](#)
33. Alam, R.; Khan, S.U.; Usman, M.; Asif, M.; Farooqi, I.H. A critical review on treatment of saline wastewater with emphasis on electrochemical based approaches. *Process Saf. Environ. Prot.* **2022**, *158*, 625–643. [\[CrossRef\]](#)
34. Wang, Z.; Zheng, J.; Tang, J.; Wang, X.; Wu, Z. A pilot-scale forward osmosis membrane system for concentrating low-strength municipal wastewater: Performance and implications. *Sci. Rep.* **2016**, *6*, 21653. [\[CrossRef\]](#)
35. Hellal, M.S.; Hemdan, B.A.; Youssef, M.; El-Taweel, G.E.; Abou Taleb, E.M. Novel electro-oxidation unit for electro-disinfection of E. coli and some waterborne pathogens during wastewater treatment: Batch and continuous experiments. *Sci. Rep.* **2022**, *12*, 16417. [\[CrossRef\]](#)
36. Darvishmotevalli, M.; Zarei, A.; Moradnia, M.; Noorisepehr, M.; Mohammadi, H. Optimization of saline wastewater treatment using electrochemical oxidation process: Prediction by RSM method. *MethodsX* **2019**, *6*, 1101–1113. [\[CrossRef\]](#)
37. Nassef, A.M.; Fathy, A.; Sayed, E.T.; Abdelkareem, M.A.; Rezk, H.; Tanveer, W.H.; Olabi, A.G. Maximizing SOFC performance through optimal parameters identification by modern optimization algorithms. *Renew. Energy* **2019**, *138*, 458–464. [\[CrossRef\]](#)
38. Olabi, A.G.; Haridy, S.; Sayed, E.T.; Radi, M.A.; Alami, A.H.; Zwayyed, F.; Salameh, T.; Abdelkareem, M.A. Implementation of Artificial Intelligence in Modeling and Control of Heat Pipes: A Review. *Energies* **2023**, *16*, 760. [\[CrossRef\]](#)
39. Sayed, E.T.; Rezk, H.; Abdelkareem, M.A.; Olabi, A.G. Artificial neural network based modelling and optimization of microalgae microbial fuel cell. *Int. J. Hydrog. Energy* **2023**. [\[CrossRef\]](#)
40. Nassef, A.M.; Sayed, E.T.; Rezk, H.; Abdelkareem, M.A.; Rodriguez, C.; Olabi, A.G. Fuzzy-modeling with Particle Swarm Optimization for enhancing the production of biodiesel from Microalgae. *Energy Sources Part A Recovery Util. Environ. Eff.* **2019**, *41*, 2094–2103. [\[CrossRef\]](#)
41. Meena, M.; Shubham, S.; Paritosh, K.; Pareek, N.; Vivekanand, V. Production of biofuels from biomass: Predicting the energy employing artificial intelligence modelling. *Bioresour. Technol.* **2021**, *340*, 125642. [\[CrossRef\]](#) [\[PubMed\]](#)
42. Rezk, H.; Nassef, A.M.; Inayat, A.; Sayed, E.T.; Shahbaz, M.; Olabi, A.G. Improving the environmental impact of palm kernel shell through maximizing its production of hydrogen and syngas using advanced artificial intelligence. *Sci. Total Environ.* **2019**, *658*, 1150–1160. [\[CrossRef\]](#) [\[PubMed\]](#)

43. Martins, M.A.F.; Rodrigues, A.E.; Loureiro, J.M.; Ribeiro, A.M.; Nogueira, I.B.R. Artificial Intelligence-oriented economic non-linear model predictive control applied to a pressure swing adsorption unit: Syngas purification as a case study. *Sep. Purif. Technol.* **2021**, *276*, 119333. [\[CrossRef\]](#)
44. Wen, H.-T.; Lu, J.-H.; Phuc, M.-X. Applying Artificial Intelligence to Predict the Composition of Syngas Using Rice Husks: A Comparison of Artificial Neural Networks and Gradient Boosting Regression. *Energies* **2021**, *14*, 2932. [\[CrossRef\]](#)
45. Rezk, H.; Olabi, A.G.; Abdelkareem, M.A.; Alami, A.H.; Sayed, E.T. Optimal Parameter Determination of Membrane Bioreactor to Boost Biohydrogen Production-Based Integration of ANFIS Modeling and Honey Badger Algorithm. *Sustainability* **2023**, *15*, 1589. [\[CrossRef\]](#)
46. Salameh, T.; Sayed, E.T.; Olabi, A.G.; Hdaib, I.I.; Allan, Y.; Alkasrawi, M.; Abdelkareem, M.A. Adaptive Network Fuzzy Inference System and Particle Swarm Optimization of Biohydrogen Production Process. *Fermentation* **2022**, *8*, 483. [\[CrossRef\]](#)
47. Rezk, H.; Ferahtia, S.; Sayed, E.T.; Abdelkareem, M.A.; Olabi, A.G. Robust parameter identification strategy of solid oxide fuel cells using bald eagle search optimization algorithm. *Int. J. Energy Res.* **2022**, *46*, 10535–10552. [\[CrossRef\]](#)
48. Chen, X.; Yi, Z.; Zhou, Y.; Guo, P.; Farkoush, S.G.; Niroumandi, H. Artificial neural network modeling and optimization of the Solid Oxide Fuel Cell parameters using grey wolf optimizer. *Energy Rep.* **2021**, *7*, 3449–3459. [\[CrossRef\]](#)
49. Olabi, A.G.; Rezk, H.; Sayed, E.T.; Ghoniem, R.M.; Abdelkareem, M.A. Boosting carbon dioxide adsorption capacity applying Jellyfish optimization and ANFIS-based modelling. *Ain Shams Eng. J.* **2023**, *14*, 101931. [\[CrossRef\]](#)
50. Chen, X.; Wu, X.; Lee, K.Y. The mutual benefits of renewables and carbon capture: Achieved by an artificial intelligent scheduling strategy. *Energy Convers. Manag.* **2021**, *233*, 113856. [\[CrossRef\]](#)
51. Zhao, L.; Dai, T.; Qiao, Z.; Sun, P.; Hao, J.; Yang, Y. Application of artificial intelligence to wastewater treatment: A bibliometric analysis and systematic review of technology, economy, management, and wastewater reuse. *Process Saf. Environ. Prot.* **2020**, *133*, 169–182. [\[CrossRef\]](#)
52. Federation, W.E.; Association, A. *Standard Methods for the Examination of Water and Wastewater*; American Public Health Association (APHA): Washington, DC, USA, 2005; p. 21.
53. Rezk, H.; Mohammed, R.H.; Rashad, E.; Nassef, A.M. ANFIS-based accurate modeling of silica gel adsorption cooling cycle. *Sustain. Energy Technol. Assess.* **2022**, *50*, 101793. [\[CrossRef\]](#)
54. Yang, Y.; Chen, H.; Heidari, A.A.; Gandomi, A.H. Hunger games search: Visions, conception, implementation, deep analysis, perspectives, and towards performance shifts. *Expert Syst. Appl.* **2021**, *177*, 114864. [\[CrossRef\]](#)
55. Un, U.T.; Altay, U.; Koparal, A.S.; Ogutveren, U.B. Complete treatment of olive mill wastewaters by electrooxidation. *Chem. Eng. J.* **2008**, *139*, 445–452. [\[CrossRef\]](#)
56. Bhatti, M.S.; Reddy, A.S.; Thukral, A.K. Electrocoagulation removal of Cr(VI) from simulated wastewater using response surface methodology. *J. Hazard. Mater.* **2009**, *172*, 839–846. [\[CrossRef\]](#)
57. Panizza, M.; Cerisola, G. Olive mill wastewater treatment by anodic oxidation with parallel plate electrodes. *Water Res.* **2006**, *40*, 1179–1184. [\[CrossRef\]](#)

Disclaimer/Publisher's Note: The statements, opinions and data contained in all publications are solely those of the individual author(s) and contributor(s) and not of MDPI and/or the editor(s). MDPI and/or the editor(s) disclaim responsibility for any injury to people or property resulting from any ideas, methods, instructions or products referred to in the content.